# Design and optimization of a novel surface plasmon resonance biosensor based on Otto configuration

**E. K. Akowuah, T. Gorman, and S. Haxha***

*Broadband and Wireless Communication group, Department of Electronics, University of Kent, Canterbury, CT2 7NT, UK*
**S.Haxha@kent.ac.uk*

**Abstract:** A theoretical study on a novel planar waveguide surface Plasmon Biosensor is presented in this paper. The proposed biosensor has a configuration similar to the Otto excitation mechanism for surface Plasmon polaritons. The performance of the device with respect to key system parameters such as gap - width and device length is investigated using an eigenmode solver with perfectly matched layers (PML). Device resolution of $2.3\times10^{-6}$ *RIU* has been demonstrated for an aqueous analyte.



**OCIS codes:** (130.6010) Sensors; (240.6680) Surface plasmons; (060.2370) Fiber optics sensors; (130.3120) Integrated optics devices.

## References and links

1. J. Homola, S. Yee, and G. Gauglitz, "Surface plasmon resonance sensors: review," Sens. Actuators B Chem. **54**(1-2), 3–15 (1999).
2. C. Mouvet, R. D. Harris, C. Maciag, B. J. Luff, J. S. Wilkinson, J. Piehler, A. Brecht, G. Gauglitz, R. Abuknesha, and G. Ismail, "Determination of simazine in water samples by waveguide surface plasmon resonance," Anal. Chim. Acta **338**(1-2), 109–117 (1997).
3. J. Homola, J. Dostálek, S. F. Chen, A. Rasooly, S. Jiang, and S. S. Yee, "Spectral surface plasmon resonance biosensor for detection of staphylococcal enterotoxin B in milk," Int. J. Food Microbiol. **75**(1-2), 61–69 (2002).
4. V. Koubová, E. Brynda, L. Karasová, J. Skvor, J. Homola, J. Dostálek, P. Tobiska, and J. Rosický, "Detection of foodborne pathogens using surface plasmon resonance biosensors," Sens. Actuat. B **74**, 100–105 (2001).
5. T. T. Goodrich, H. J. Lee, and R. M. Corn, "Direct detection of genomic DNA by enzymatically amplified SPR imaging measurements of RNA microarrays," J. Am. Chem. Soc. **126**(13), 4086–4087 (2004).
6. X. D. Hoa, A. G. Kirk, and M. Tabrizian, "Towards integrated and sensitive surface plasmon resonance biosensors: a review of recent progress," Biosens. Bioelectron. **23**(2), 151–160 (2007).
7. J. Dostálek, J. Ctyroký, J. Homola, E. Brynda, M. Skalský, P. Nekvindová, J. Spirková, J. Skvor, and J. Schröfel, "Surface plasmon resonance biosensor based on integrated optical waveguide," Sens. Actuat. B **76**, 8–12 (2001).
8. R. C. Jorgenson, and S. S. Yee, "A fiber-optics chemical sensor based on surface plasmon resonance," Sens. Actuators B Chem. **12**(3), 213–220 (1993).
9. M. Niggemann, A. Katerkamp, M. Pellmann, P. Bolsmann, J. Reinbold, and K. Cammann, "Remote sensing of tetrachloroethene with a micro-fibre optical gas sensor based on surface plasmon resonance spectroscopy," Sens. Actuators B Chem. **34**(1-3), 328–333 (1996).
10. R. Slavík, J. Homola, and E. Brynda, "A miniature fiber optic surface plasmon resonance sensor for fast detection of Staphylococcal enterotoxin B," Biosens. Bioelectron. **17**(6-7), 591–595 (2002).
11. A. J. C. Tubb, F. P. Payne, R. B. Millington, and C. R. Lowe, "Single-mode optical fibre surface plasma wave chemical sensor," Sens. Actuators B Chem. **41**(1-3), 71–79 (1997).
12. L. A. Obando, and K. S. Booksh, "Tuning dynamic range and sensitivity of white-light, multimode, fiber-optic surface plasmon resonance sensors," Anal. Chem. **71**(22), 5116–5122 (1999).
13. A. Hassani, B. Gauvreau, M. Fassi Fehri, A. Kabashin, and M. Skorobogatiy, "Photonic crystal fiber and waveguide-based surface plasmon resonance sensors for application in the visible and Near-IR," Electromagnetics **28**(3), 198 (2008).
14. T. Allsop, R. Neal, C. Mou, P. Brown, S. Saied, S. Rehman, K. Kalli, D. J. Webb, J. Sullivan, D. Mapps, and I. Bennion, "Exploitation of multilayer coatings for infrared surface plasmon resonance fiber sensors," Appl. Opt. **48**(2), 276–286 (2009).
15. R. Jha, R. K. Verma, and B. D. Gupta, "Surface Plasmon Resonance-Based Tapered Fiber Optic Sensor: Sensitivity Enhancement by Introducing a Teflon Layer Between Core and Metal Layer," Plasmonics **3**(4), 151–156 (2008).
16. H. P. Ho, W. Yuan, C. L. Wong, S. Y. Wu, Y. K. Suen, S. K. Kong, and C. L. Lin, "Sensitivity enhancement based on application of multi-pass interferometry in phase-sensitive surface plasmon resonance biosensor," Opt. Commun. **275**(2), 491–496 (2007).

#115920 - $15.00 USD Received 15 Sep 2009; revised 18 Nov 2009; accepted 22 Nov 2009; published 8 Dec 2009

17. R. Jha, and A. K. Sharma, "High-performance sensor based on surface plasmon resonance with chalcogenide prism and aluminum for detection in infrared," Opt. Lett. **34**(6), 749–751 (2009).
18. P. Debackere, S. Scheerlinck, P. Bienstman, and R. Baets, "Surface plasmon interferometer in silicon-on-insulator: novel concept for an integrated biosensor," in *3rd International Conference on Group IV Photonics*(IEEE, Ottawa, CANADA, 2006), pp. 7–9.
19. S. A. Maier, "Plasmonics: Fundamentals and Applications," Springer, New York, 40 – 52 (2007)
20. A. D. Boardman, "Electromagnetic surface modes," Wiley, Chichester (1982).
21. E. Kretschmann, and H. Raether, "Radiative decay of nonradiative surface plasmons excited by light," Z. Naturforsch. A **23**, 2135–2136 (1968).
22. R. D. Harris, and J. S. Wilkinson, "Waveguide surface Plasmon resonance sensors," Sens. Actuators B Chem. **29**(1-3), 261–267 (1995).
23. R. Ramaswamy, and R. Srivastava, "Ion exchanged glass waveguides: a review," J. Lightwave Technol. **6**(6), 984–1000 (1988).
24. P. Noutsios, and G. L. Yip, "Characterization and modeling of planar surface and buried glass waveguides made by field-assisted K^+ ion exchange," Appl. Opt. **31**(25), 5283–5291 (1992).
25. H. de Bruijn, R. Kooyman, and J. Greve, "Choice of metal and wavelength for surface-plasmon resonance sensors: some considerations," Appl. Opt. **31**(4), 440_1–442 (1992).
26. M. L. Nesterov, A. V. Kats, and S. K. Turitsyn, "Extremely short-length surface plasmon resonance devices," Opt. Express **16**(25), 20227–20240 (2008).
27. C. Jung, S. Yee, and K. Kuhn, "Integrated-Optics Wave-Guide Modulator Based On Surface-Plasmon Resonance," J. Lightwave Technol. **12**(10), 1802–1806 (1994).
28. R. Levy, and S. Ruschin, "Design of a Single-Channel Modal Interferometer Waveguide Sensor," IEEE Sens. J. **9**(2), 146–153 (2009).
29. CAMFR, http://camfr.sourceforge.net.
30. P. Yeh, "Optical Waves in Layered Media," Wiley, New York, (1988).
31. J. Chilwell, and I. Hodgkinson, "Thin-films field-transfer matrix theory of planar multilayer waveguides and eflection from prism-loaded waveguides," J. Opt. Soc. Am. A **1**(7), 742–753 (1984).
32. A. Ghatak, K. Thyagarajan, and M. Shenoy, "Numerical analysis of planar optical waveguides using matrix approach," J. Lightwave Technol. **5**(5), 660–667 (1987).
33. R. Syms, and J. Cozens, Optical Guided Waves and Devices, McGraw-Hill, London, (1992).
34. P. B. Johnson, and R. W. Christy, "Optical-Constants of Noble-Metals," Phys. Rev. B **6**(12), 4370–4379 (1972).
35. B. Gauvreau, A. Hassani, M. Fassi Fehri, A. Kabashin, and M. A. Skorobogatiy, "Photonic bandgap fiber-based Surface Plasmon Resonance sensors," Opt. Express **15**(18), 11413–11426 (2007).

## 1. Introduction

The concept of Surface Plasmon Resonance (SPR) has been increasingly exploited for development of optical biosensors. SPR biosensors have found extensive application in the analysis of biomolecular interactions (BIA) and detection of chemical and biological analytes [1], where they provide benefits of real-time, sensitive and label-free technology. They have been used for detection of various chemical and biological compounds in areas such as environmental protection [2], food safety [3], [4] and medical diagnostics [5].

Currently, most commercial SPR biosensors are generally based on the traditional prism-coupled SPR configuration, which is simple, robust and highly sensitive. However, they are not amenable to miniaturization and integration [6]. There has been a growing interest in the development of robust, portable and highly sensitive SPR sensing devices capable of out of laboratory measurements. Recent progress in sensitive fiber and waveguide SPR, SPR on silicon material and multi – analyte SPR systems present options for miniaturisation and integration of SPR sensor systems [6].

Waveguide based SPR sensors aim to provide highly integrated, multichannel and robust sensing devices [6]. They have the ability to accommodate multiple sensing elements on a single platform or substrate, as these structures may be micro-fabricated in parallel or in series where wavelength division multiplexing techniques can be used to extract the signal from the different sensing elements [6]. This allows the integration of a reference signal which allows the effect of environmental changes (temperature changes, noise source) to be nullified [6,7].

Early development in fiber optic SPR sensors include a plastic-clad silica fiber with partly removed cladding [8,9], a side-polished optical fiber [10], a tapered single-mode fiber [11] and a tip-polished fiber [12]. Some recent advances include photonic crystal fiber and waveguide SPR sensors [13], lapped D-shaped fiber sensors [14] and tapered fibre optic sensors [15].In addition, concepts such as multi-pass interferometry in phase-sensitive SPR sensors [16] and the development of sensors based on chalcogenide prism and aluminum,

#115920 - $15.00 USD Received 15 Sep 2009; revised 18 Nov 2009; accepted 22 Nov 2009; published 8 Dec 2009

provide options in realization of high performance SPR biosensors [17]. However, the integration of fiber - SPR to other biosensor components raises some design issues. Among these issues include the high precision requirement for the insertion of the fiber into a planar substrate containing fluidic circuit and chambers and the requirement of additional optical components to achieve efficient coupling of light in and out of the fiber [6].

The proposed alternative approach to fiber-based SPR has been the planar optical waveguide structure. Thin-film technologies have long been used to develop planar optical waveguides consisting of a multilayer structure of varying optical refractive index that can support a propagating light mode.

Regarding recent trends in integration and miniaturisation of SPR biosensors, *Debackere et al* [15] proposed a highly integrated and sensitive SPR interferometer sensor based on silicon – on – insulator technology [18]. The basic element of that sensor was a Surface Plasmon interferometer consisting of a thin layer of gold embedded in a silicon membrane. It was demonstrated that the sensor could achieve a resolution of $1\times10^{-6}$ *RIU*. The reported sensitivity was however obtained by intensity modulation, which has been proved to be less robust to environmental noise [1]. In the same paper, it was also demonstrated that the device could achieve a sensitivity of 463.5nm / *RIU* with regards to wavelength interrogation [15].

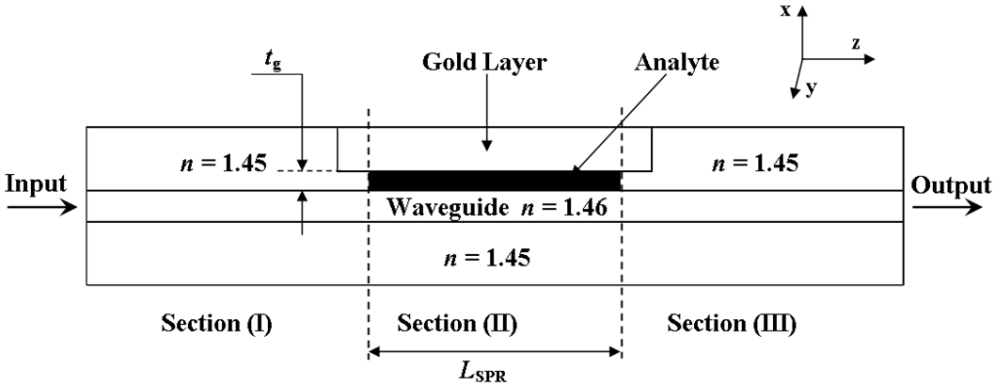


Fig. 1. Cross section of the proposed waveguide SPR sensor showing various sections.

In this paper, we propose a novel planar waveguide SPR sensor based on the Otto [19] configuration. The proposed waveguide SPR sensor as shown in Fig. 1, has the analyte placed between the core and gold layer. The configuration of this sensor does not require any matching layer and therefore, makes the design very simple. We intend to demonstrate that the proposed sensor, can achieve a high sensitivity of 4300 nm / *RIU*. Recent advances in microfabrication and thin – film technology makes the fabrication of our proposed sensor design feasible.

A brief theory regarding waveguide SPR sensors is given in the next section, which will be followed by the discussion of simulation results and finally conclusions and future work presented in the last section.

## 2. Theory

A surface plasma wave (SPW) is an electromagnetic wave which propagates along the boundary between a dielectric and a metal [1]. The propagation constant of an SPW, $\beta$, can be expressed as:

$$\beta = \frac{\omega}{c}\sqrt{\frac{\varepsilon_M \varepsilon_D}{\varepsilon_M + \varepsilon_D}} \tag{1}$$

where $\omega$, is the angular frequency, $c$ the speed of light in vacuum, $\varepsilon_D$ and $\varepsilon_M$ are the dielectric functions of the dielectric and metal, respectively [20]. Equation (1) describes a surface

#115920 - $15.00 USD Received 15 Sep 2009; revised 18 Nov 2009; accepted 22 Nov 2009; published 8 Dec 2009

Plasmon wave if the real part of $\varepsilon_M$ is negative and $|\varepsilon_M| < |\varepsilon_D|$ [1]. This condition is fulfilled by several metals at optical wavelengths, of which gold is most commonly employed in SPR sensors [1]. The real and imaginary parts of the propagation constant $\beta$, represent the spatial periodicity and attenuation of the SPW in the direction of propagation, respectively [20].

The electromagnetic field of the SPW is confined at the metal – dielectric boundary and decreases exponentially into both media, with the vast majority of the field concentrated in the dielectric [1]. This makes the propagation constant of the SPW extremely sensitive to changes in the refractive index of the dielectric. Surface Plasmon Resonance (SPR) sensors operate on this basic principle.

In SPR biosensors, an SPW is excited by a light wave, whose wave vector parallel to the metal surface matches that of the SPW [1]. These biosensors have biomolecular recognition elements on the surface of the metal, which recognise and capture analyte present in a fluid, leading to a local increase in the refractive index at the metal surface. This results in an increase in the propagation constant of the surface plasmon wave (SPW) propagating along the metal surface. The interaction of the light wave with the SPW can alter the light's characteristics such as amplitude, phase, polarisation and spectral distribution. Changes in these characteristics can be correlated with changes in the propagation constant of the SPW [1].

One of the requirements for the excitation of an SPW is that the x – component (x-y plane) of the incident light wave vector ($k_x$), matches that of the SPW ($k_{sp}$) [1]. This can be achieved by means of prism coupling, waveguide coupling and grating coupling [1].

In the prism coupling technique, a light wave passes through a high refractive index prism and is totally reflected at the prism-metal interface, generating an evanescent wave penetrating the metal layer. The propagation constant of this wave can be adjusted to match that of the SPW by controlling the angle of incidence. The wave vector of this evanescent wave is given by [19]

$$k_x = k_0 \sqrt{\varepsilon_p} \times \sin\theta \tag{2}$$

where $k_0 = \frac{2\pi}{\lambda}$, $\varepsilon_p$ is the permittivity of the prism, $\theta$ is the angle of incidence of the light wave, the wave vector of the SPW is given by

$$k_{sp} = k_0 \times n_{eff} \tag{3}$$

In Eq. (3), $n_{eff}$ represents the effective index of the SPW.

There are two main configurations with regards to the prism coupling technique. The most common configuration is the Kretschmann method [21], in which a thin metal film is evaporated on top of a glass prism. By tuning the angle of incidence of the totally reflected beam inside the prism to an appropriate value, the surface plasmon resonance condition is established [19]. In the Kretschmann configuration, the evanescent wave created at the metal – glass interface has to penetrate the metal layer in order to excite a surface plasmon at the metal – air interface. If the metal is too thin, the SPW will be strongly damped because of radiation damping into the glass. On the other hand, if the metal is too thick, the SPW can no longer be efficiently excited due to absorption in the metal. Hence, the thickness of the metal plays a critical role in the excitement of SPW [19].

In the Otto configuration, the tail of the evanescent wave at the glass – air interface is brought into contact with a metal – air interface that supports SPW. For a sufficiently large gap - width, the evanescent wave is only weakly influenced by the presence of the metal. By selecting a suitable angle of incidence of the totally reflected beam inside the prism, a surface plasmon resonance condition is established [19]. For a small gap - width, the resonance is broadened and shifted due to radiation damping of the SPW whilst a large gap - width leads to inefficient excitation of SPW or no SPR condition [19]. The surface Plasmon resonance

#115920 - $15.00 USD Received 15 Sep 2009; revised 18 Nov 2009; accepted 22 Nov 2009; published 8 Dec 2009

condition in both Kretschmann and Otto configurations manifest itself as a minimum in the reflected light.

The Kretschmann configuration has been the preferred configuration over the years, as the Otto configuration proved to be experimentally inconvenient due the challenging control of the tiny air gap between the interfaces [19].

Recent advances in microfabrication and thin – film technology makes the fabrication of SPR biosensors based on Otto configuration feasible. We believe that it is feasible to fabricate SPR waveguide sensors based on Otto configuration with typical gap - widths exceeding 100 nm, as presented in this paper, with current microfabrication and thin – film technology. Among other applications, SPR biosensors based on the Otto configuration will be preferable in applications where direct contact with the metal surface is undesirable [19].

### *2.1 Planar Waveguide SPR Biosensors*

Planar waveguide technologies offer the possibility of producing compact, monolithic, multisensory devices which may be connected to instrumentation using optical fibres, allowing remote operation [22].

Most planar waveguide sensors have three major sections. These are the input, multilayer and output sections. The input and output sections are employed to couple light into and out of the multilayer region of the device. The multilayer metal – clad part of the device acts as the interaction zone with the analyte.

There are several structural variables to optimise in order to design a planar waveguide SPR biosensor. However, there are some practical constraints regarding the substrate material, and subsequent waveguide manufacture, the availability of practical buffer layer materials and metal for the sensor surface [22]. It has been demonstrated that the use of a low index substrate glass offers the easiest phase matching between waveguide and surface Plasmon modes in a device when operating in water [23,24].

Another method for altering the phase-matching conditions is to insert a low refractive index buffer layer between the waveguide and metal. This serves a dual purpose of increasing the propagation distance of the surface plasmons [23] and shifting the location of the peak modal losses with respect to the refractive index of superstrate (analyte) [23]. The final material variable is the metal film. The choice of metal for use in SPR devices has been discussed in [25]. The stability and inertness of the metal film to aqueous environment is of paramount importance when designing sensors for such an environment [22]. It is for this reason that most SPR sensors use gold for the metallic layer.

In addition to the material variables, the dimension of the components is also very important. Specifically, the metal thickness, the length of the multi – layer section, buffer thickness and a host of other dimensional variables influence the operation of the sensor. Optimisation of these variables has been extensively discussed in [26,22,27,28].

## 3. Simulation Results

Figure 1 shows the schematic of the proposed waveguide SPR biosensor. Similar to the conventional waveguide SPR sensors, the proposed design has an input (I) and output (III) waveguide sections with a multilayer (II) section in the middle.

The input and output sections (I and III) consist of core and cladding with refractive indices of 1.46 and 1.45 respectively. The thickness of the core and cladding are fixed at 1μm and 2μm respectively, to ensure single mode operation [27]. In the SPR section (II) of the proposed device, the analyte is sandwiched between the gold and core layers as shown in Fig. 2, similar to the Otto configuration. The length of the SPR section is denoted as $L_{SPR}$ whilst the thickness of the analyte layer is given as $t_g$.

Simulations were carried out using CAMFR, an eigenmode solver with perfectly matched layers (PML) [29]. This ensures the absorption of waves travelling towards the walls, without the introduction of additional reflections, regardless of wavelength, incidence angle or polarisation of the incident wave [29]. The simulation results obtained by CAMFR were verified by benchmarking them against results from a commercial Finite Element software

#115920 - $15.00 USD Received 15 Sep 2009; revised 18 Nov 2009; accepted 22 Nov 2009; published 8 Dec 2009

package [30], [31], and [32]. The relatively high memory requirement and longer computation time of FEM for analysis of the proposed sensor resulted in the choice of CAMFR as the computation tool.

Each section of the sensor is modelled as a multilayer system and CAMFR is used to solve eigenmodes supported therein. The optical power transmitted through the structure in Fig. 1 is calculated by analysing the modal coupling between the various sections of the sensor. Sections (I) and (III) are assumed to be identical and lossless. The modal expansion coefficients are calculated using the necessary overlap integrals after the modes in Sections (I) and (II) are located [33]. These modes are then propagated through the length of Section (II) of the sensor before being coupled into Section (III), enabling the power transmitted to be calculated. The permittivity of gold was modelled using data from Johnson and Christy [34].

A broadband (550nm – 850nm) TM polarized light is applied at the input section of the sensor, and the transmission characteristics of the entire system are observed for variation in $L_{SPR}$ and $t_g$. The refractive index of the analyte ($n_{analyte}$) is assumed to be 1.33 (aqueous environment).

We begin the analysis by investigating the effects of the gap - width ($t_g$) on the performance of the sensor. The gap - width ($t_g$) is varied from 175nm to 300nm, whilst that of the SPR section ($L_{SPR}$) is kept constant at 100 μm. The transmission response of the proposed waveguide SPR sensor for various values of $t_g$ is shown in Fig. 2.

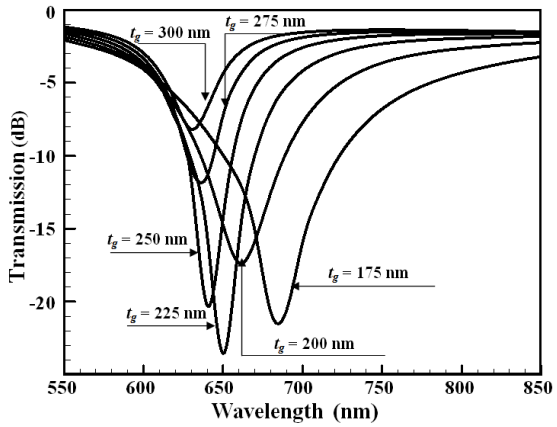


Fig. 2. Transmission properties of the proposed waveguide SPR sensor for various $t_g$ values. $n_{analyte}$ = 1.33 and $L_{SPR}$ = 100μm.

The minimum in the various curves shown in Fig. 2 indicate the surface plasmon resonance condition in the respective curves. The resonant wavelengths for each curve can be located at the minimum of the respective curves. The minimum in the received light at resonance condition can be attributed to the fact that a portion of the input light is converted to SPW travelling at the gold – analyte interface, such that its energy is totally dissipated before reaching the output section of the sensor. The minimum can also be thought of as being due to destructive interference between the input light and that of the SPW due to radiation damping. It can therefore be established that the magnitude of the dip in the received power is influenced by the efficiency of the SPW conversion, which is dependent on the gap - width, $t_g$. This explains the dependency of the transmission on the gap – width ($t_g$) of the sensor at a fixed $L_{SPR}$. Comparing the various plots in Fig. 2 reveals that gap - widths ($t_g$) of 225 nm, 250 nm, 175 nm and 150 nm lead to comparably high dips in the received power. Since the gap – width ($t_g$), is filled with the analyte, it has an influence on the phase - matching conditions between the waveguide and surface plasmon modes. This implies a change in the gap – width ($t_g$), leads to a corresponding change in the phase – matching conditions, specifically the resonant wavelength ($\lambda_{res}$). Figure 2 illustrates this property where a shift in the resonant

#115920 - $15.00 USD Received 15 Sep 2009; revised 18 Nov 2009; accepted 22 Nov 2009; published 8 Dec 2009

wavelength is observed for a change in the gap – width ($t_g$). This property is very important for the design of the device at a specified resonant wavelength.

The performance of SPR sensors can be characterised by three main parameters: sensitivity, resolution and FWHM. The sensitivity ($S_n$) of a SPR sensor with spectral interrogation is defined as [1]

$$S_n = \frac{\delta\lambda_{res}}{\delta n_{analyte}} \tag{4}$$

where $\delta n_{analyte}$ is the change in analyte refractive index and $\delta\lambda_{res}$ is the corresponding shift in resonance wavelength. This relation has been used to calculate the sensitivities of the proposed SPR sensor for different values of $t_g$ as shown in Fig. 3. The sensitivity was calculated based on the change in refractive index of the analyte ($n_{analyte}$) from 1.33 to 1.34.

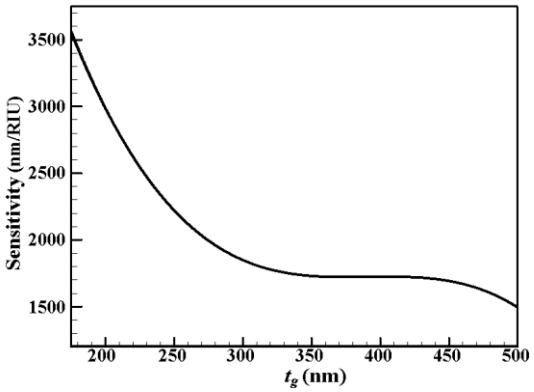


Fig. 3. Sensitivity of the proposed SPR sensor for various $t_g$ values. $L_{SPR}$ = 100μm.

It can be observed that the sensitivity of the proposed sensor varies from a peak value of 3750 nm/RIU at $t_g$ = 175 nm and decreases with increase in $t_g$ . This behavior can be attributed to the inefficient excitation of the SPW as the gap – width ($t_g$) is increased [19].

The resolution of an SPR sensor can be determined by [1]:

$$s_n^{-1} \times \delta\lambda_a \tag{5}$$

where $\delta\lambda_a$ is the sensitivity of the device used to measure the shift in resonant wavelength of the sensor (typically 0.01nm). The full width at half maximum power (FWHM), determines how accurately $\delta\lambda_{res}$ can be determined. A large FWHM value decreases the accuracy in the measurement of the SPR wavelength ($\delta\lambda_{res}$). Figure 4 shows the variation in FWHM of the proposed SPR sensor with regards to $t_g$.

#115920 - $15.00 USD Received 15 Sep 2009; revised 18 Nov 2009; accepted 22 Nov 2009; published 8 Dec 2009

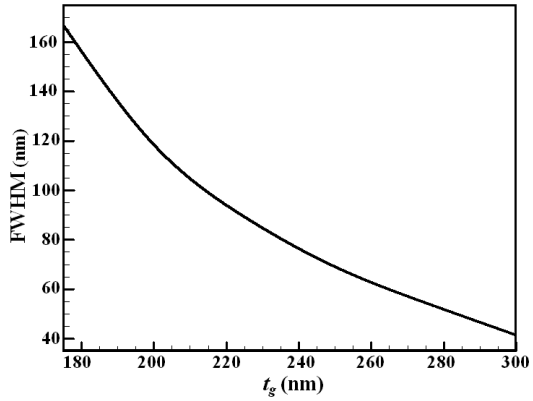


Fig. 4. FWHM of the proposed SPR sensor for various $t_g$ values. $L_{SPR}$ = 100μm and $n_{analyte}$ = 1.33.

It can be observed that for a fixed $L_{SPR}$, the FWHM varies inversely proportionally to $t_g$. By combining results from Fig. 3 and 4, optimal structural parameters can be obtained for a fixed $L_{SPR}$ value depending on whether high sensitivity or low FWHM value is the priority of the design objective. In most cases, however, a compromise must be reached such that the sensitivity is maximised whilst minimising the FWHM.

An optimum length of the SPR section of the device will ensure that the SPW will have enough travel distance to dissipate into the gold metal before reaching the detector at the output [26,22,27]. Hence, it is important to investigate the effect of the length of the SPR ($L_{SPR}$) section on the performance of the proposed sensor. In this regard, $t_g$ is fixed at different specific values whilst that of $L_{SPR}$ is varied from 100 μm to 500 μm. The response of the device to variation in $L_{SPR}$ for $t_g$ = 250 nm is shown in Fig. 5.

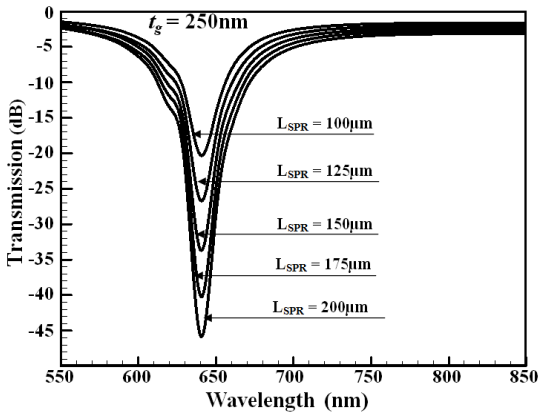


Fig. 5. Transmission characteristics of the proposed SPR sensor for different $L_{SPR}$ values ($t_g$ = 250 nm).

It can be observed that the dip in the various curves increase with an increase in $L_{SPR}$. This could be attributed to increase in the attenuation of the SPW in the gold layer and that of the light wave in the waveguide. Another observation worth noting is that of the constant position of the resonant wavelength regardless of $L_{SPR}$. If one considers the resonance wavelength to be the point of phase matching between the waveguide mode and the surface-plasmon wave then it is expected to be independent of $L_{SPR}$. This explains the phenomenon of constant resonant wavevength irrespective of $L_{SPR}$ as shown in Fig. 5. This behavior is very important for the design of short length sensors.

#115920 - $15.00 USD Received 15 Sep 2009; revised 18 Nov 2009; accepted 22 Nov 2009; published 8 Dec 2009

Next, the effect of $L_{SPR}$ on the sensitivity of the proposed sensor is investigated for different values of $t_g$. Figure 6 shows the particular case for $t_g$ = 175 nm and 225 nm.

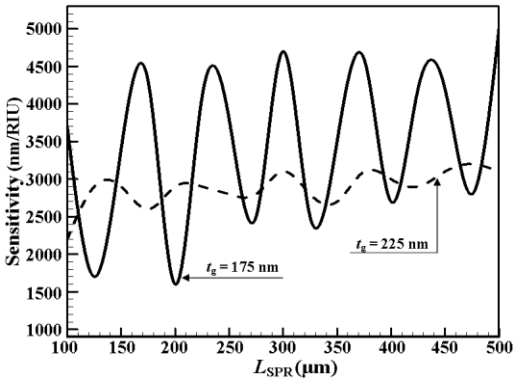


Fig. 6. Variation in sensitivity of the proposed SPR sensor for varying $L_{SPR}$ values. The thick line and dashes correspond to $t_g$ values of 175 nm and 225 nm respectively.

It is shown in Fig. 6 that the sensitivity of the sensor is dependent on $L_{SPR}$ . In the case of $t_g$ = 175 nm, the sensitivity varies from a value of 3700 nm/RIU to 5000 nm/RIU. Similar sensitivity variation can be observed for the scenario of $t_g$ = 225 nm. When a guided mode enters the active region of the sensor, it is decomposed into guided and radiation modes of the region, the power distribution among these modes being dependent on the field profiles of the modes and thus the physical structure of the active section [19,26]. At relatively small gap – width ($t_g$) values, the structure of the active region permits the existence of more complex modes such that the sensitivity of the sensor is highly dependent on $L_{SPR}$ as shown in Fig. 5. However, as the gap – width ($t_g$) is increased, the dependency decreases and the sensitivity curve becomes more flattened. This property is illustrated in Fig. 5 where the degree of dependency for the case of $t_g$ = 225nm is relatively smaller as compared to that of 175 nm.

The next step involves investigating the effects of the $L_{SPR}$ on the FWHM of the proposed SPR sensor. This is illustrated in Fig. 7.

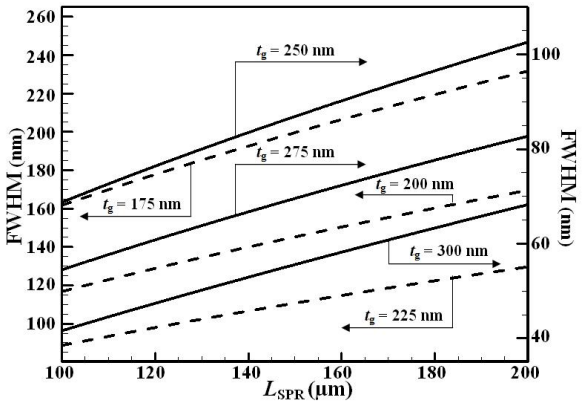


Fig. 7. Variation in FWHM of the proposed SPR sensor for varying $L_{SPR}$ values ($n_{analyte}$ = 1.33.).

The results presented so far, give a good understanding of the effects of the structural parameters on the performance of the proposed sensor. One can choose a combination of structural parameters to optimise the sensor given specific requirements such high sensitivity, low FWHM or both. In our particular case, we intend to optimise the sensor to operate in an aqueous environment with the best possible sensitivity and an acceptable FWHM value.

It can be observed from Fig. 7 that the scenarios depicted in thick continuous lines ($t_g$ = 250nm, 275nm and 300nm) lead to low FWHM values as compared to those in dashes ($t_g$ =

#115920 - $15.00 USD Received 15 Sep 2009; revised 18 Nov 2009; accepted 22 Nov 2009; published 8 Dec 2009

175nm, 200nm and 225 nm). Despite their comparatively low FWHM values, they yield relatively low sensitivities. Based on our design objectives, the optimal parameters for maximum sensitivity and minimum FWHM in aqueous environment are $t_g$ = 175 nm and $L_{SPR}$ = 175 μm.

The next step investigates the resonant wavelength ($\lambda_{res}$) as a function of $n_{analyte}$ of the optimised device. The results are shown in Fig. 8.

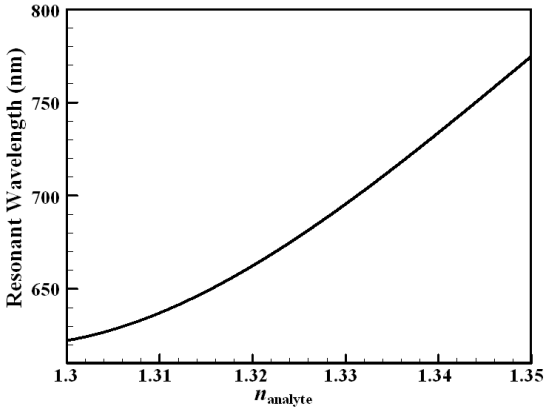


Fig. 8. Variation in the resonant wavelength with respect to $n_{analyte}$ ($t_g$ = 175nm, $L_{SPR}$ = 175μm).

The maximum slope of the curve in Fig. 8 represents the sensitivity of the device, which is found to be 4300 nm/*RIU* with a resolution of $2.3\times10^{-6}$ *RIU*. The FWHM is calculated to be approximately 213 nm.

Figure 9 illustrates the shift in resonant wavelength for a small change in analyte refractive index of the proposed sensor. The sensitivity of the sensor can also be computed using Fig. 9 and this leads to a value of 4300 nm/*RIU*, which is in agreement with that of Fig. 8.

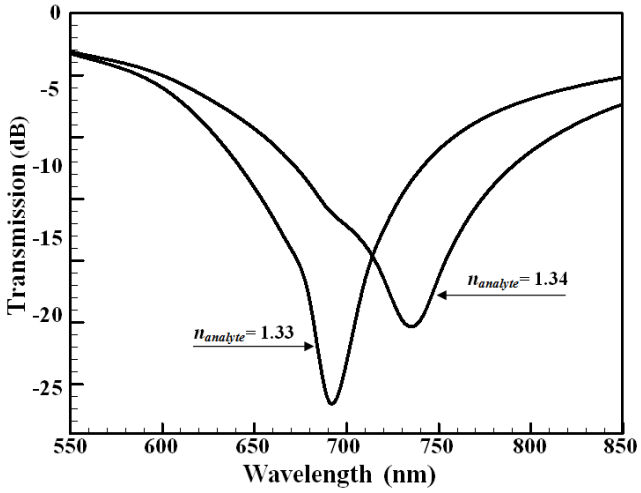


Fig. 9. Shift in resonant wavelength with respect to $n_{analyte}$ ($t_g$ = 175 nm, $L_{SPR}$ = 175μm).

## 4. Conclusion

The design and optimisation of a novel waveguide SPR biosensor based on the Otto configuration, has been presented in this paper. The structure is very simple in nature and does not require any buffer layer. It has been shown that by selecting appropriate structural parameters, the sensor can achieve a sensitivity of 4300 nm/*RIU* (resolution of $2.3\times10^{-6}$ *RIU*

#115920 - $15.00 USD Received 15 Sep 2009; revised 18 Nov 2009; accepted 22 Nov 2009; published 8 Dec 2009

with regards to wavelength interrogation) and a FWHM of 213 nm. With regards to sensitivity, the performance of the proposed sensor is comparable to [8–11] in addition to the waveguide SPR sensors reviewed in [6]. Furthermore, the sensitivity of the proposed sensor is comparatively higher than the spectral interrogation sensitivity reported in [18], which is based on silicon – on insulator technology.

Regarding fabrication issues, we believe that it is feasible to fabricate the proposed SPR waveguide sensor since gap - widths ($t_g$) exceed 150 nm, which is large enough to be fabricated with current microfabrication and thin – film technology. In addition, *Gauvreau et al* proposed and fabricated a waveguide SPR sensor based on photonic bandgap. Since the fabrication of the sensor in [35] with a more complicated design was feasible, we are very optimistic that our simple design should be even more feasible.

Among other applications, SPR biosensors based on the Otto configuration will be preferable in applications where direct contact with the metal surface is undesirable [19].

#115920 - $15.00 USD Received 15 Sep 2009; revised 18 Nov 2009; accepted 22 Nov 2009; published 8 Dec 2009